Supplementary Information (SI) for Journal of Materials Chemistry A.

Supporting Information

Design and large-scale preparation of the high-soft laminated elastic fabric with cascading fibrous cluster structure for wearable smart bandage

Heng Zhang [a*], Ke Zhao [a], Qian Zhai [a], Xiaoyu Guan [b], Jingqiang Cui [c], Qi Zhen [d]

a. College of Intelligent Textile and Fabric Electronics, Zhongyuan university of technology, No. 1 Huaihe road, Xinzheng county, 451191, Zhengzhou, Henan province, China.

b. School of materials designing and engineering, Beijing institute of fashion technology, Beijing, 100029, Beijing, China.

c. Henan Tuoren medical device Co., Ltd, No. 1 Yangze road, Changyuan county, 453400, Xinxiang, Henan province, China.

d. College of fashion technology, Zhongyuan university of technology, No. 1 Huaihe road, Xinzheng county, 451191, Zhengzhou, Henan province, China.

*** Corresponding Author**

Heng Zhang, Ph.D., College of Intelligent Textile and Fabric Electronics, Zhongyuan University of Technology **E-mail:** m-esp@163.com, zhangheng2699@zut.edu.cn. **Tel:** +86-156 3902 5712.

Address: Zhongyuan university of technology, No.1 Huaihe road, Xinzheng, Zhengzhou city, Henan province, China.

Supporting Information

Figures

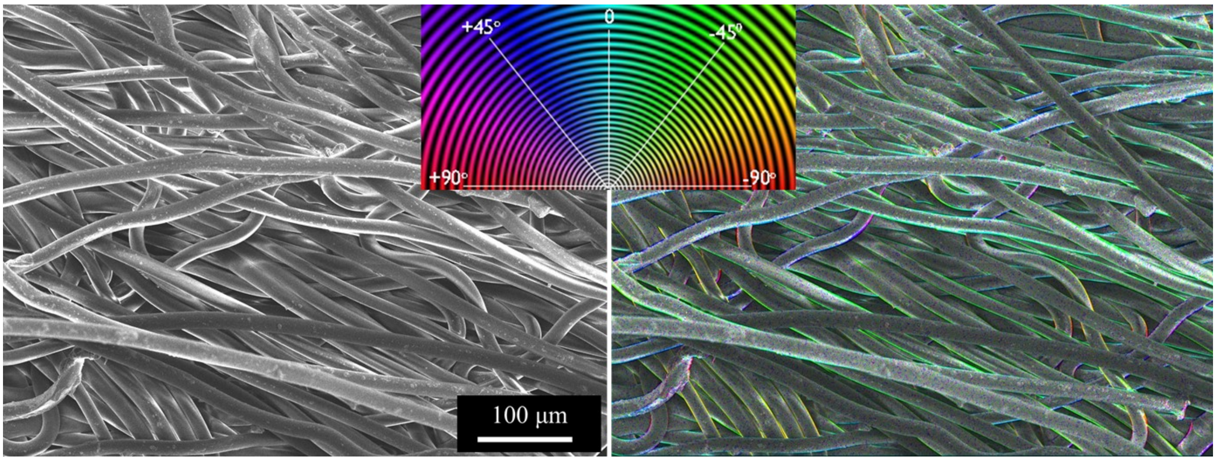

Fig. S1. SEM images (left) and its orientation colour map (right) of the PBE filaments webs. The Orientation colour map were obtained by analysing the SEM images by a free software named OrientationJ (ImageJ plugin, Switzerland, http://bigwww.epfl.ch/demo/orientation/). The colour representation reflects the different orientations.

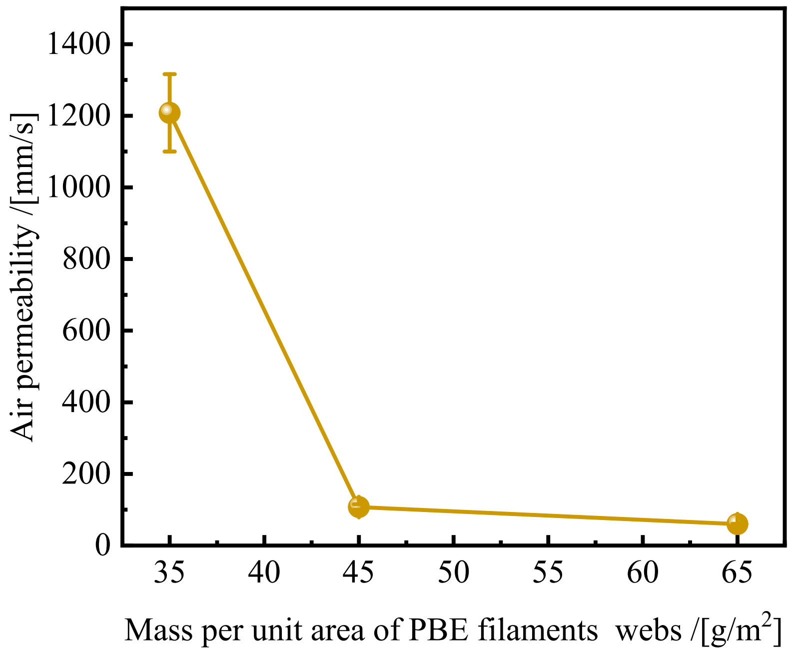

Fig. S2. The air permeability of PBE filaments webs with different mass per unit area.

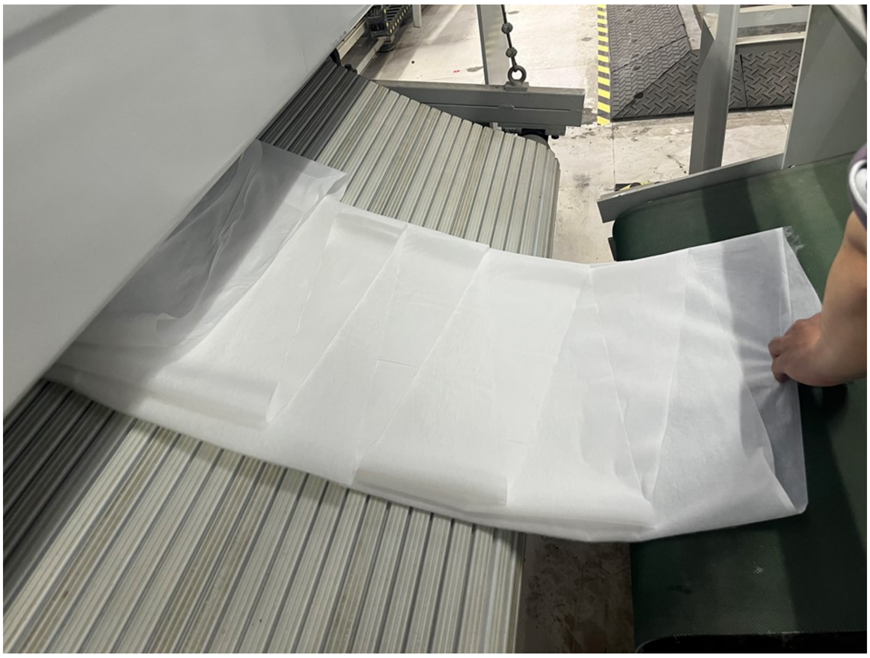

Fig. S3. The photograph of the PBE filaments webs after the cross-lapping process.

Fig. S4. The photograph of the alginic (left), cellulose (middle), and low melt polylactic acid/ polylactic acid bicomponent fibers (right).

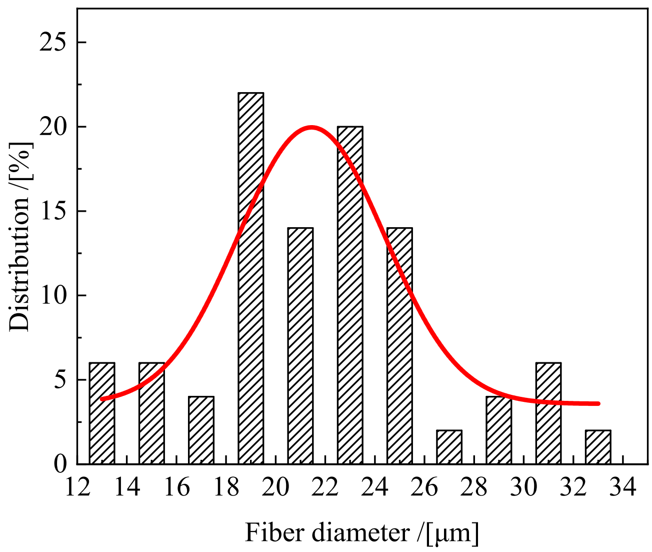

Fig. S5. The fiber diameter distribution of the laminated elastic fabric.

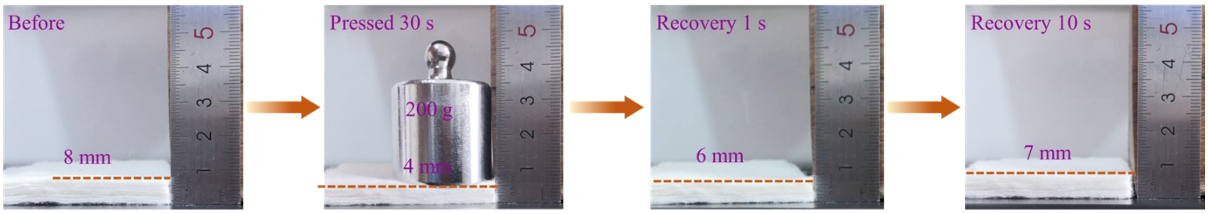

Fig. S6. The photograph of compression recovery rate testing of the prepared samples of laminated elastic fabric named MR-FL 40.3.

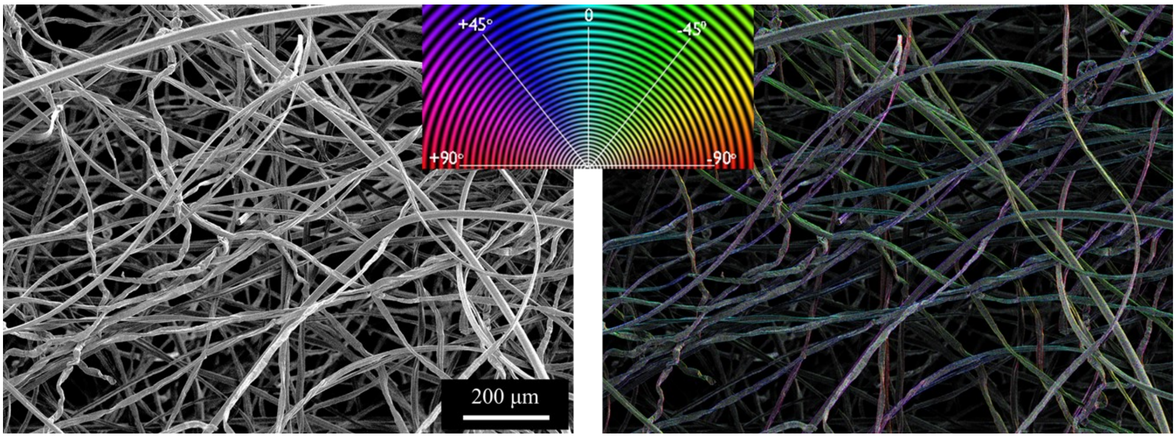

Fig. S7. SEM images (left) and its orientation colour map (right) of the fluffy layer. The Orientation colour map were obtained by analysing the SEM images by a free software named OrientationJ (ImageJ plugin, Switzerland, http://bigwww.epfl.ch/demo/orientation/). The colour representation reflects the different orientations.

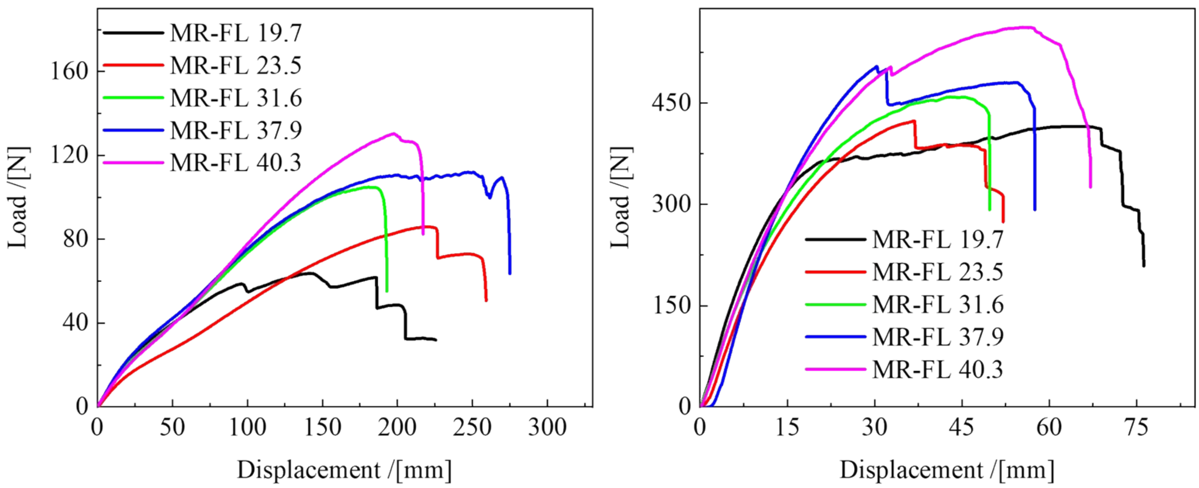

Fig. S8. Load-displacement curves of the samples of laminated elastic fabric prepared at needle-punching density of 245.8 punches/cm^2 during the tensile testing. (Left - machine direction, Right - cross direction)

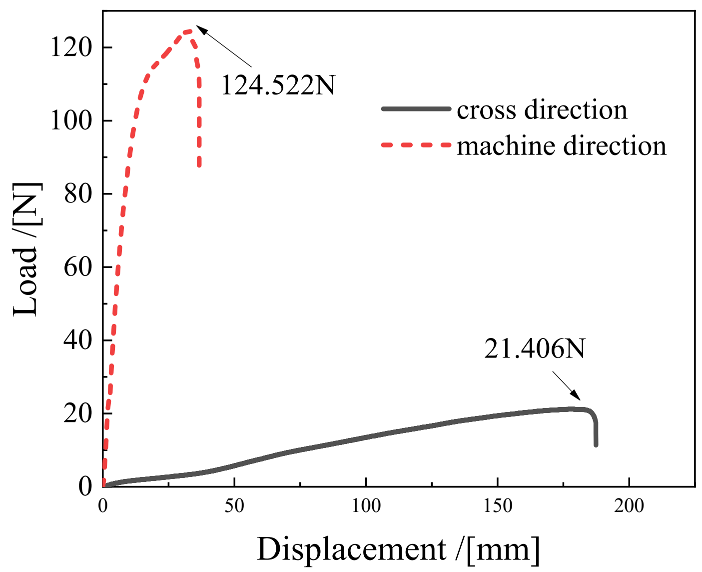

Fig. S9. Load-displacement curves of the samples of PBE filaments webs with mass per unit area of 45 g/m^2 during the tensile testing.

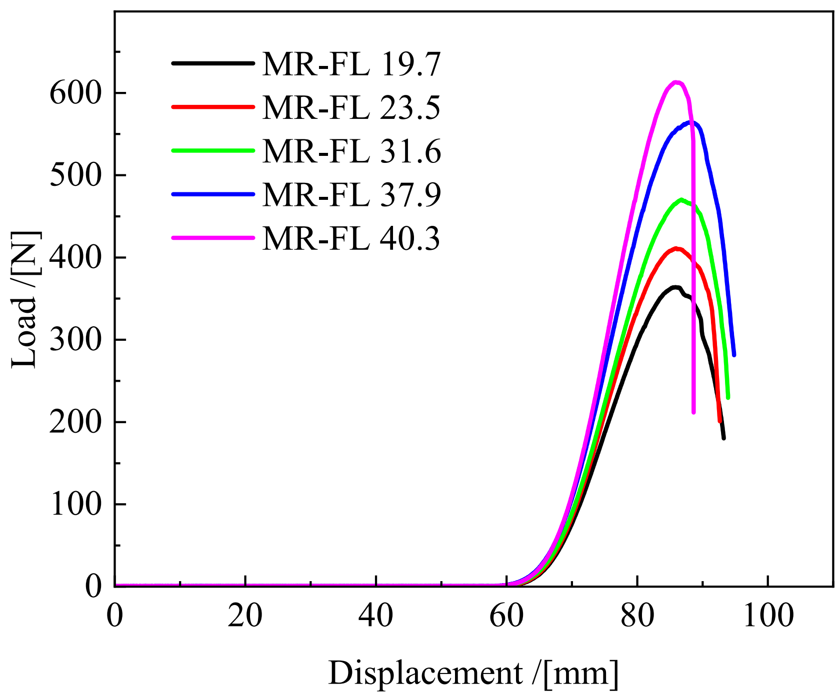

Fig. S10. Load-displacement curves of the samples of laminated elastic fabric prepared at needle-punching density of 245.8 punches/cm^2 during the burst testing.

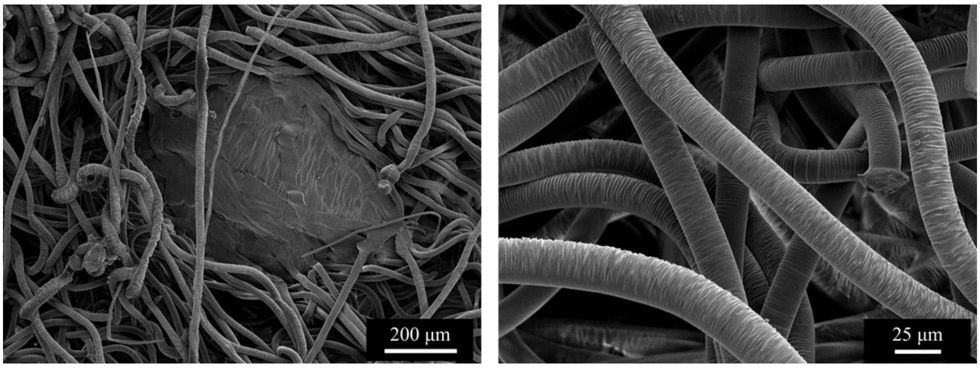

Fig. S11. The SEM images of the sample of PBE filaments webs after stretching.

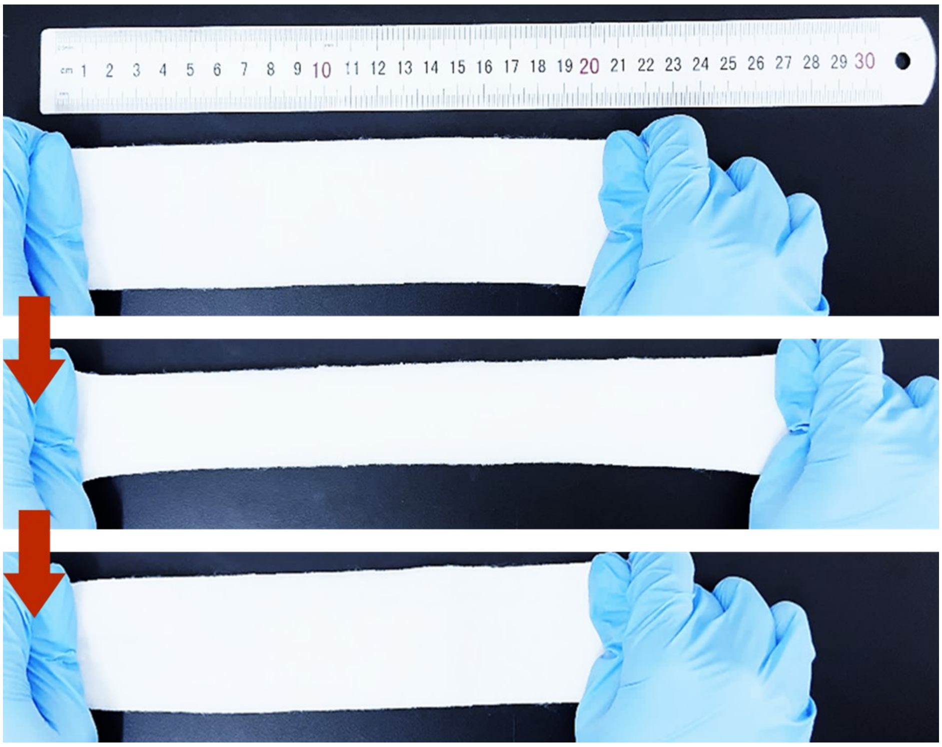

Fig. S12. The photograph of the ensile elastic behaviour of the prepared samples of laminated elastic fabric named MR-FL 40.3.

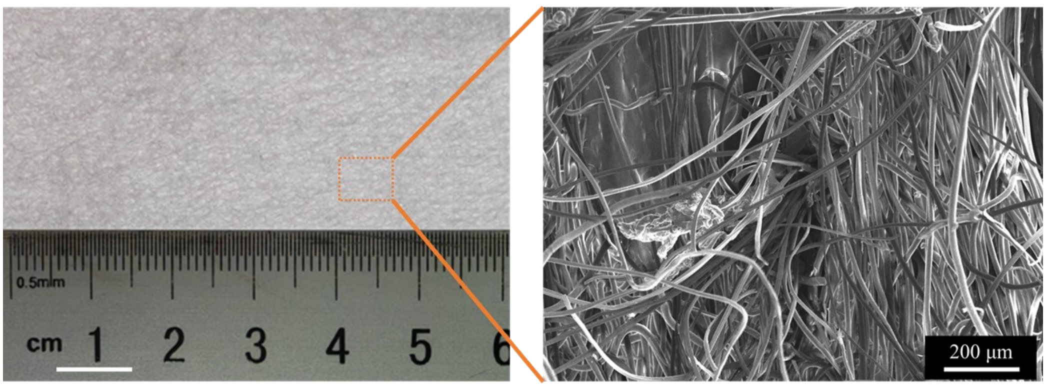

Fig. S13. The photograph (left) and SEM images (right) of the prepared samples of laminated elastic fabric named MR-FL 40.3 after stretching.

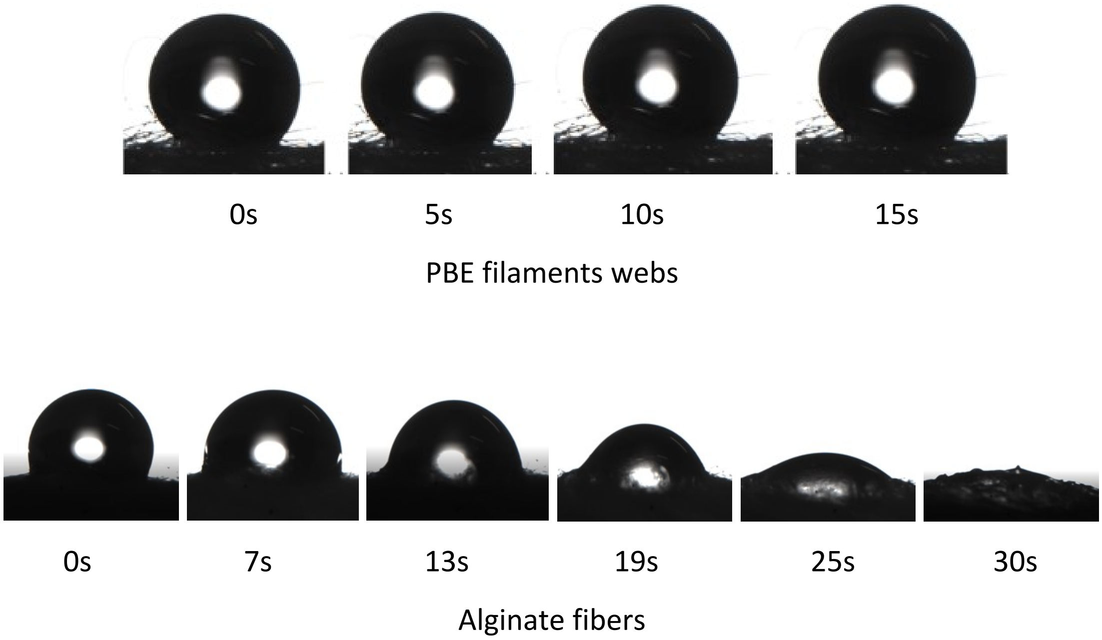

Fig. S14. Liquid water contact angle of the PBE filaments webs and Alginate fibers. The liquid water contact angles testing was achieved by a liquid contact angle testing system (SDC-350, Dongguan Shengding Precision Instruments Co., Ltd., China). The testing liquid was stroke-physiological saline solution.

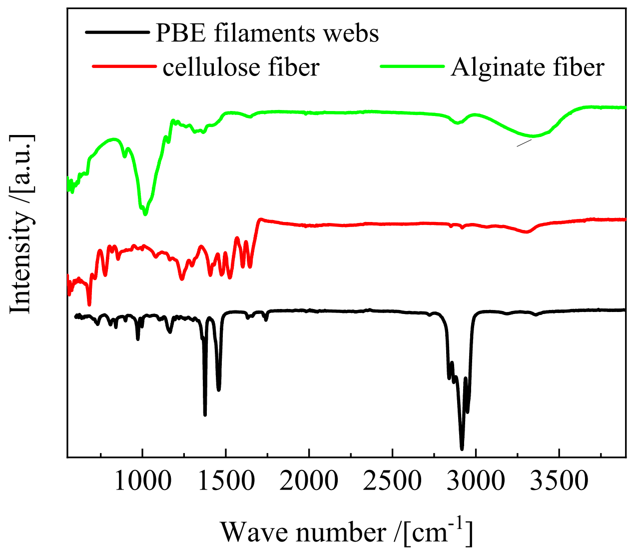

Fig. S15. The fourier transform infrared spectra of the PBE filaments webs, cellulose fibers and alginate fibers. The fourier transform infrared spectra was obtained by a total reflection spectrometer (TENSOR 37, Bruker, Germany).

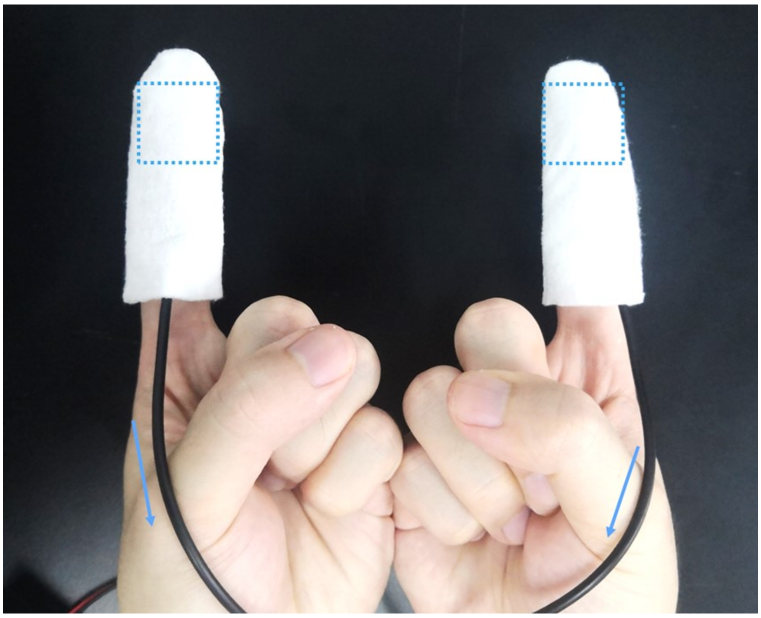

Fig. S16. The photograph of the fingerstall embedded by a sensor.

(Prior to participation, each individual was provided with a detailed explanation of the study purpose, procedures and potential risks. Participants had the opportunity to ask questions and were assured that their participation was voluntary and that they could withdraw at any time without any consequences.)

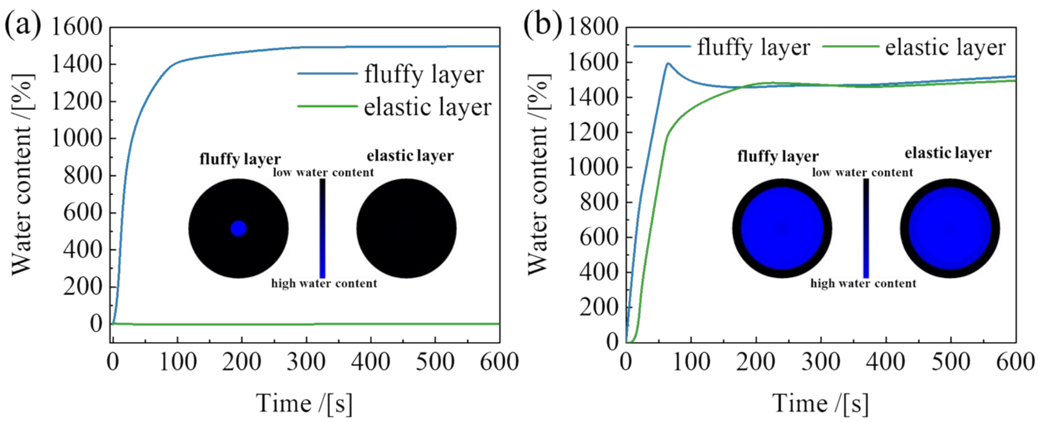

Fig. S17. Unidirectional sweat transfer capability of laminated elastic fabrics (MR-FL 40.3). (a) water entered through the samples from fluffy layer, (b) water entered through the samples from elastic layer.

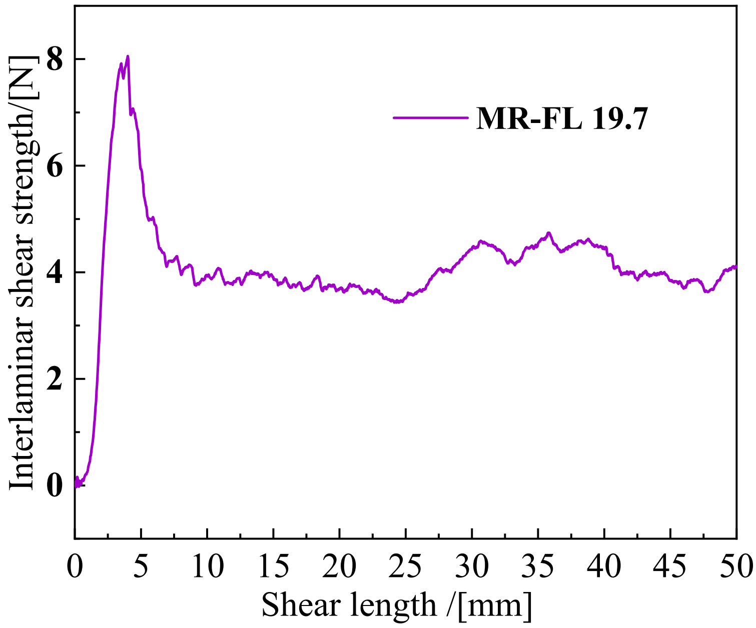

Fig. S18. The interlaminar shear strength of laminated elastic fabrics

Tab. S1 The mechanical properties of PBE filament webs

/	tensile breaking strength /[N]	Breaking elongation /[%]	Elastic recovery /[%]
MD	47.9±0.41	83.7±11.71	81.6±3.51
CD	15.1±0.46	249.0±5.76	71.3±5.42

Tab. S2 The mechanical performance parameters of laminated compression elastic fabrics under different washing times (MR-FL 40.3)

/	MD		CD	
Washing times/[-]	tensile breaking strength /[N]	Elastic recovery /[%]	tensile breaking strength /[N]	Elastic recovery /[%]
0	111.9±4.5	75.3±2.1	547.1±3.8	69.0±1.5
50	107.3±7.2	74.8±1.8	543.1±6.1	68.6±1.8
100	105.4±5.6	74.3±1.2	539.1±5.7	67.9±1.4
200	104.8±5.6	73.7±2.3	534.1±4.2	66.8±2.1